Disorder-induced enhancement of local hexatic correlations in two-dimensional fluids

N Shankaraiah[1], Surajit Sengupta[1], Gautam I Menon[2,3,4]

[1] TIFR Centre for Interdisciplinary Sciences, 36/p Gopanpally, Hyderabad 500107, India
[2] Department of Physics, Ashoka University, P.O.Rai, Sonepat 131029, India
[3] The Institute of Mathematical Sciences, C.I.T Campus, Taramani, Chennai 600113, India
[4] Homi Bhabha National Institute, Training School Complex, Anushaktinagar, Mumbai 400094, India

E-mail: naddis@tifrh.res.in, surajit@tifrh.res.in and gautam.menon@ashoka.edu.in

Abstract
Quenched disorder affects translational and orientational correlations in two-dimensional interacting particle systems. Such disorder always suppresses orientational order in crystalline states. Surprisingly, in fluid phases of particles interacting with a power-law repulsive interaction, increasing the strength of a quenched Gaussian random pinning potential appears to enhance hexatic order locally. We propose that nearby pairs of pinned particles lock in the relative orientation of neighbours around them, propagating hexatic orientational order across larger distances than in the unpinned fluid. We test this idea using Monte Carlo simulations of interacting particles in their fluid phase in two dimensions, where two of the particles are constrained to be permanently pinned at a fixed distance from each other. We use Voronoi tesselations of instantaneous particle configurations to demonstrate that these pinned particles create hexatic neighbourhoods that can extend well beyond the range of their separation. This structuring is enhanced when the particle density is increased and is most prominent in the vicinity of the liquid-solid transition. Testing these ideas experimentally using experiments on 2D colloidal systems should be feasible.

Keywords: colloids, quenched disorder, Hexatics, orientational correlations, 2D liquids

(Some figures may appear in colour only in the online journal)

1. Introduction

A true crystalline state with long-ranged translational order cannot exist at any non-zero temperature in two dimensions [1]. Low temperature phases with the long-ranged orientational order that accompanies crystallinity are, however, stable. Renormalization group approaches suggest that such an orientationally ordered phase should first melt, via a continuous transition, into a phase with quasi-long-ranged orientational order [1–5]. Subsequently, this 'hexatic' phase is expected to undergo a separate continuous transition into the disordered liquid [2–5]. Both orientational and translational order are short-ranged in the liquid state, decaying exponentially over length scales of a few inter-particle spacings [6].

The remarkable possibility of a two-step continuous melting transition driven by the unbinding of topological defects has ensured that particle systems in reduced dimensions continue to remain a focus of theoretical and experimental attention [6–26].

While such two-stage melting [2–5] is now increasingly seen in large-scale, well-equilibrated simulations of particles interacting through simple power-law or hard-core potentials, it is now believed that these two separate transitions need not both be continuous. In one scenario, the melting transition from crystal to hexatic is proposed to be continuous but the subsequent hexatic to isotropic liquid transition to be first-order [27]. An equilibrium hexatic phase has been seen in a number of systems [28–32]. Alternate proposals, involving a

direct, one-step first-order crystal to liquid melting transition, have also been discussed [33, 34]. The core energies for topological defects such as dislocations and disclinations, quantities that depend on the pair potential between particles, are now understood to play a role in deciding the nature of these transitions [35–43].

The question of phases and phase transitions in low-dimensional systems in the presence of disorder is particularly relevant to the interpretation of experimental data. Such disorder is typically both quenched and random. The term 'quenched' indicates that the disorder enters through the specification of additional variables in the Hamiltonian that are not dynamical i.e. they do not fluctuate in time. If, in addition, these variables are random, they can be simply accounted for by specifying a probability distribution that generates them. For particles moving on a underlying two-dimensional substrate, the substrate presents an effective one-body potential to the particles. A disordered substrate can be modelled as a one-body potential, generated by a probability distribution with vanishing mean and specified two-point correlations, that acts on the particles.

Real-space imaging experiments [44], in which the trajectories of colloidal particles can be recorded in time over a large field, now enable both equal time and unequal time correlations in such systems to be measured to high accuracy. Such experiments have renewed interest in measurements that were infeasible earlier. These include the accurate characterization of multi-particle correlations in the fluid phase of particle systems in a two-dimensional quenched disordered background [12]. Experimentally, substrates that present a pre-determined pinning potential to the particles can be engineered. A useful representation of a disordered substrate is in terms of a random potential landscape governed by Gaussian statistics [12, 45]. Such a landscape is fully characterised at the level of its two-point correlations. For interacting particles in this landscape, the measurable quantities of interest are usually the lowest-order distribution functions, since these can often be compared to theoretical predictions.

In a disordered fluid, the local time-averaged density $\rho(\mathbf{r})$ is itself inhomogeneous in any single realization of the disorder. Translational invariance is restored on disorder averaging [11, 12, 46], yielding the uniform density of the liquid, i.e.

$$\rho_\ell = [\langle \rho(\mathbf{r}) \rangle], \tag{1}$$

where the brackets $[\cdot]$ denote a disorder averaging over the probability distribution from which individual disorder configurations are generated and $\langle \cdot \rangle$ denotes, as usual, the thermal average.

Similarly, while the conventional two-point correlation function

$$g(\mathbf{r}, \mathbf{r}') = \frac{1}{\rho_0^2} \left[\langle \rho(\mathbf{r}) \rho(\mathbf{r}') \rangle \right] \tag{2}$$

is a function of both locations $\mathbf{r}$ and $\mathbf{r}'$ prior to disorder averaging, the disorder-averaged quantity $g_r^{(1)}(r)$ defined as [10, 11, 46]

$$g_r^{(1)}(r) = \frac{1}{\rho_0^2} \left[\langle \rho(r) \rho(0) \rangle \right] - \frac{\delta(r)}{\rho_0}, \tag{3}$$

is a function of the magnitude of the radial separation of the two points only.

Another interesting correlation function can be defined in a disordered system. This is the disorder-averaged correlation of the time-averaged densities. Such a density correlation function, $g_r^{(2)}(r)$, is defined as

$$g_r^{(2)}(r) = \frac{1}{\rho_0^2} \left[\langle \rho(r) \rangle \langle \rho(0) \rangle \right]. \tag{4}$$

This is qualitatively different from $g_r^{(1)}(r)$. It is best thought of as an analogue of the Edwards–Anderson correlation function defined and studied for disordered spin systems.

Some years ago, we showed that Monte Carlo simulations and liquid state theory approaches could be used to calculate $g_r^{(1)}(r)$ and $g_r^{(2)}(r)$ for model two-dimensional particle systems in a quenched disordered background [10, 11]. More recently, we have investigated versions of these correlation functions that describe the persistence of orientational order in the fluid [46]. The appropriate disorder-averaged orientational correlation functions are defined using the local hexatic order parameter,

$$\psi_6^j = \frac{1}{n_j} \sum_{k=1}^{n_j} \exp(\mathrm{i}6\theta_{jk}), \tag{5}$$

where n_j counts the number of nearest neighbours of particle j. The quantity θ_{jk} is the angle between the vector from particle j to its nearest neighbour k and the unit vector defining the reference x-axis. The associated orientational correlation function is [46]

$$g_\theta^{(1)}(r) = \left[\langle \psi_6(\vec{r}) \psi_6^*(0) \rangle \right], \tag{6}$$

where $\psi_6(\vec{r}) = \sum_{i=1}^{N} \delta(\vec{r} - \vec{r}_i) \psi_6^i$.

The analog of $g_r^{(2)}(r)$ for orientational correlations is defined [46] via

$$g_\theta^{(2)}(r) = \left[\langle \psi_6(\vec{r}) \rangle \langle \psi_6^*(0) \rangle \right]. \tag{7}$$

For simplicity we will refer to correlations that are simply the disorder-averaged correlation functions in the pure system as 'diagonal' correlation functions, whereas the Edwards–Anderson [47] correlation functions, non-trivial in the disordered fluid, will be referred to as 'off-diagonal' correlation functions. These reflect the way such correlations are defined using replica methods [10].

From these earlier studies, we concluded the following [46]: we found that off-diagonal orientational correlations increased with the strength of quenched disorder in the range of densities where the pure system was a liquid. For the higher densities appropriate to a crystal, $g_\theta^{(2)}(r)$ decreased with disorder at large r. This suggested that quenched disorder might enhance orientational correlations in a liquid while destroying it in a crystal. We obtained a re-entrant behavior, where $g_\theta^{(2)}(r)$

at large r first increased and then decreased as the disorder strength was increased.

We attributed this to a 'lock-in' mechanism aligning local orientational correlations along the axes joining well-pinned particles, possibly also aided by the presence nearby of a metastable or even stable hexatic phase [46]. Our simulations showed that the local neighbourhood of individual particles, defined in terms of the mean number of particles surrounding a central particle, seemed to vary relatively weakly with disorder within the fluid phase. This supported our broad picture of the importance of an alignment of local orientational correlations along the axes joining well-pinned particles. These arguments also indicated why such off-diagonal orientational correlations might increase with the strength of quenched disorder in the fluid phase. However, our earlier work [46], while conjecturing this as an explanation for our results, did not explore this specific possibility further.

This paper tests this idea in the following way. We can characterize the neighbourhood of any fixed particle through Voronoi tesselations [48] of instantaneous configurations of all particles, including those neighbouring the fixed particle. Such tesselations provide a ideal way of analysing the instantaneous configurations of particles in terms of the orientations of the neighbouring shells of particles. By superimposing a large number of Voronoi tesselations we can investigate whether orientational order about well-pinned particles might lead to a fixed configuration of the cage of other particles about them, even though the overall system is, on average, fluid-like.

We find here that the influence of a pair of particles penetrates to several neighbour shells about them, structuring hexatic order out to such scales. We conclude that the presence of pairs of well-pinned particles that are not too far away from each other structure their orientational neighbourhood and that the effect of such pinned pairs persists out to much larger scales. We suggest that this provides a plausible explanation for the anomalous behavior of $g_\theta^{(2)}(r)$, at short to intermediate scales, as a function of increasing disorder.

This paper is organized as follows. In the next section (section 2) we summarize the correlation functions studied in this work, describing in detail the model system used for this study. Section 3 presents our results. Last, in section 4 we outline our conclusions.

2. Model and method

We largely follow the simulation procedures indicated in our previous paper [46]. We summarize them here for completeness. Our model potential energy [11, 46] is given by,

$$H_{int} = \epsilon \sum_{i<j} \left(\frac{\sigma_0}{r_{ij}} \right)^{12} + \sum_i V_d(r_i). \quad (8)$$

The first term represents the interactions between pairs of particles. We implement a cutoff for this interaction, setting it to zero if the particles are separated by a distance larger than a

cutoff of $r_c = 2.5\sigma_0$. We scale all lengths in terms of $\sigma_0 = 1$. The energy scale is set by taking $\epsilon = 1$.

The second term represents the quenched disorder potential $V_d(r)$. We generate this random potential following a method described by Chudnovsky and Dickman [45]. This one-body potential has zero mean and exponentially decaying short-range correlations in space, given by [45],

$$C_V(r) = \left[\langle V(x)V(y) \rangle_{|x-y|=r} \right] / \sigma^2 = \exp(-r/\xi). \quad (9)$$

The variance of the Gaussian distribution σ^2 defines the disorder strength which we set to $\sigma^2 = 0.55$. We choose $\xi = 0.12$, so that the disorder is effectively uncorrelated across an interparticle spacing.

Our averaging procedures are as described in [11, 12]. We use periodic boundary conditions across a rectangular box of dimensions L_x, L_y. The number of particles N_p is chosen so as to allow for the formation of a perfect triangular lattice within the box. Our particle densities are thus $\rho_0 = N_p/(L_x \times L_y)$.

We perform metropolis Monte Carlo (MC) temperature quench-and-hold simulations in two dimensions. We set the temperature $T = 1$, driving the transition from liquid to solid by changing the density. The number of particles for the simulations presented here are $N_p = 1020$. We exclude an initial 10^5 MCS in all cases to ensure equilibration. We then average over $t' = 10^4$ configurations, each separated by 10^2 MCS. In cases where we are required to average over disorder we use 20 realizations. For the pure case, we average over 2×10^5 such independent configurations. Our MC simulations at $T = 1$ obtain a freezing density $\rho_0 \sim 0.986$, in good agreement with results from earlier work [49].

We define nearest neighbours in the first shell using a cutoff criterion. The location of the first minimum in $g_r^{(1)}(r)$ is taken as the cutoff distance for counting a particle as a nearest neighbour. We define the nearest neighbours in the second shell using a similar cutoff criterion, where we identify particles present at distances between the location of the first minima in $g_r^{(1)}(r)$ to the location of the second minima in $g_r^{(1)}(r)$ as belonging to a second neighbour shell. A similar definition, involving particles at a distance between the location of the second minima to the location of the third minima in $g_r^{(1)}(r)$ are counted as belonging to the third neighbour shell.

For the pure system, to examine structuring around pinned particles, we study the orientational neighbourhood of two pinned particles, placed at a fixed distance from one another. We also study the orientational neighbourhood of a single pinned particle, to check that our simulations reproduce the expected lack of any persistent structuring about it. To do this, we perform Voronoi tesselations across an ensemble of particle configurations in equilibrium. We use these to construct distribution functions of orientational order centred around the pinned particles [48].

Voronoi tesselations divide a plane into regions that are closest to each of a given set of points, in this case the instantaneous locations of particles. For a perfect triangular lattice, all Voronoi cells are hexagons, indicative of the six-fold
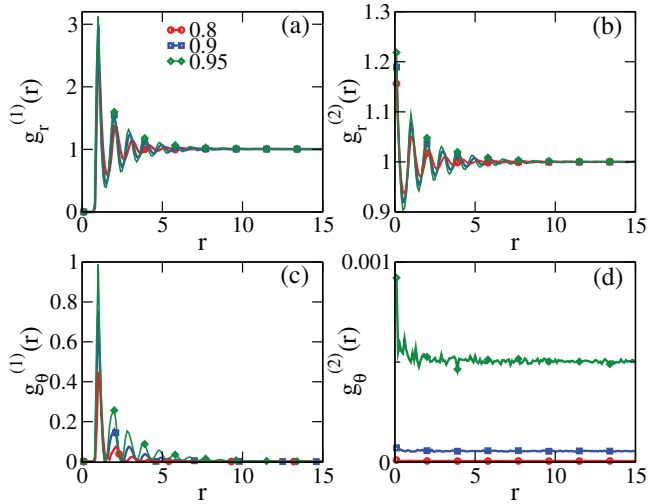
Figure 1. *Diagonal and off-diagonal correlations for various densities (ρ_0): the disorder-averaged translational correlations (a) $g_r^{(1)}(r)$ and (b) $g_r^{(2)}(r)$ as a function of r. The orientational correlations (c) $g_\theta^{(1)}(r)$ and (d) $g_\theta^{(2)}(r)$ as a function of r. The densities are $\rho_0 = 0.8, 0.9$ and 0.95.*

symmetry of the triangular lattice. For a perfectly fluid phase, one expects that while a single snapshot will provide a partition of the space into a unique set of polygons describing the instantaneous orientational neighbourhood of each particle, averaging over a large number of snapshots should remove all traces of such structure. In contrast, if the neighbourhood of a particle retains some memory of its orientational structure across the timescales of the simulation or experiment, traces of local ordering should persist even after averaging. To perform this averaging, we divide the simulation box into small square sub-boxes of width $dx = dy = 0.1$, counting the vertices of the tesselation within each box. We repeat this procedure for 2×10^5 independent configurations to obtain the averaged Voronoi tessellations by summing over vertex densities across such boxes.

We monitor θ_{jk}, the angle between the particle j to its nearest neighbour k and the unit vector defining the reference x-axis, obtaining normalized probability distributions $P(\theta)$ for the single pin and two pins with a separation $r = a, \ldots, 5a$, across the densities $\rho = 0.8, 0.9, 0.95$.

3. Results and discussion

3.1. Orientational and translational correlations in a disordered fluid

We begin by reproducing our central results for the diagonal and off-diagonal correlations $g_r^{(1)}(r)$, $g_r^{(2)}(r)$, $g_\theta^{(1)}(r)$ and $g_\theta^{(2)}(r)$ as defined in section 1 and computed as discussed in section 2. Our results for these correlation functions are presented in figure 1. We present results for three particle densities $\rho_0 = 0.8, 0.9$ and 0.95 in the fluid regime, and for a disorder strength $\sigma^2 = 0.55$. We restrict ourselves to these density values because our interest here is in orientational structuring in the correlated fluid phase, where we can be

assured that we are measuring structure and correlations in thermal equilibrium. Thus we deliberately exclude from our analysis the disordered solid phase as well as a potential thin sliver of hexatic phase that might be present in close proximity to the freezing transition.

The diagonal correlation function for densities, $g_r^{(1)}(r)$ closely resembles that in the pure system, as shown in figure 1(a). It is only weakly affected by the disorder. The off-diagonal translational correlation $g_r^{(2)}(r)$, shown in figure 1(b), decays rapidly to unity. Its oscillations are amplified at increasing density and the peak at $r = 0$ enhanced.

The envelope of the diagonal correlation function for orientations, $g_\theta^{(1)}(r)$, shown in figure 1(c) decays exponentially to zero. This is as found in the liquid phase of the pure system. The off-diagonal orientational correlations, monitored through $g_\theta^{(2)}(r)$ and shown in figure 1(d), are small and close to zero for density $\rho_0 = 0.8$. This correlation function appears to fluctuate asymptotically around a numerically small yet non-zero value for the larger densities $\rho_0 = 0.9$ and $\rho_0 = 0.95$ as shown. These results recapitulate observations in [46]. This suggests that hexatic order is promoted by quenched disorder, since such a correlation function should rightfully have vanished in the pure fluid phase. Numerically, given our choice of N, we are restricted to maximum particle separations of about 15 inter-particle spacings, so we can only conclude that disorder appears to promote medium-range hexatic order but cannot make conclusive statements about the asymptotic nature of such hexatic correlations.

3.2. The orientational neighbourhood of pinned particles: Voronoi tesselations

In this section, we present results for the averaged Voronoi tessellations as discussed in section 2 and the normalized probability distributions of the angle θ across the first, second, and third neighbour shells. Our results are summarized in figures 2–4 respectively.

We consider the pure system without disorder ($V_d = 0$ in equation (8)), simulating particle configurations in the neighbourhood of one or two permanently pinned particles, as described in section 2. A first set of results are shown in figures 2 and 3. The averaged Voronoi tessellations for densities $\rho_0 = 0.8, 0.95$ with either a single pinned particle or two pinned particles separated by $r = a, 2a, 3a, 4a$ and $5a$ are shown in (a), and (b)–(f) respectively in these two figures.

For a single pinned particle, we expect that sufficient averaging should yield an isotropic neighbourhood of particles, although we expect a density modulation about that particle. These are captured through the $g_r(r)$ for the pure system at that density. However, once we introduce two particles, the axis formed by the line connecting them breaks the isotropy. Note the strong $\pi/3$ orientations, seen as red, for the two pin case that are apparent at separation $r = a$. This structuring of local orientations decreases in amplitude as the separation of the pinned particles is increased. At separations of $r > 4a$, the modulation can be represented simply as the sum
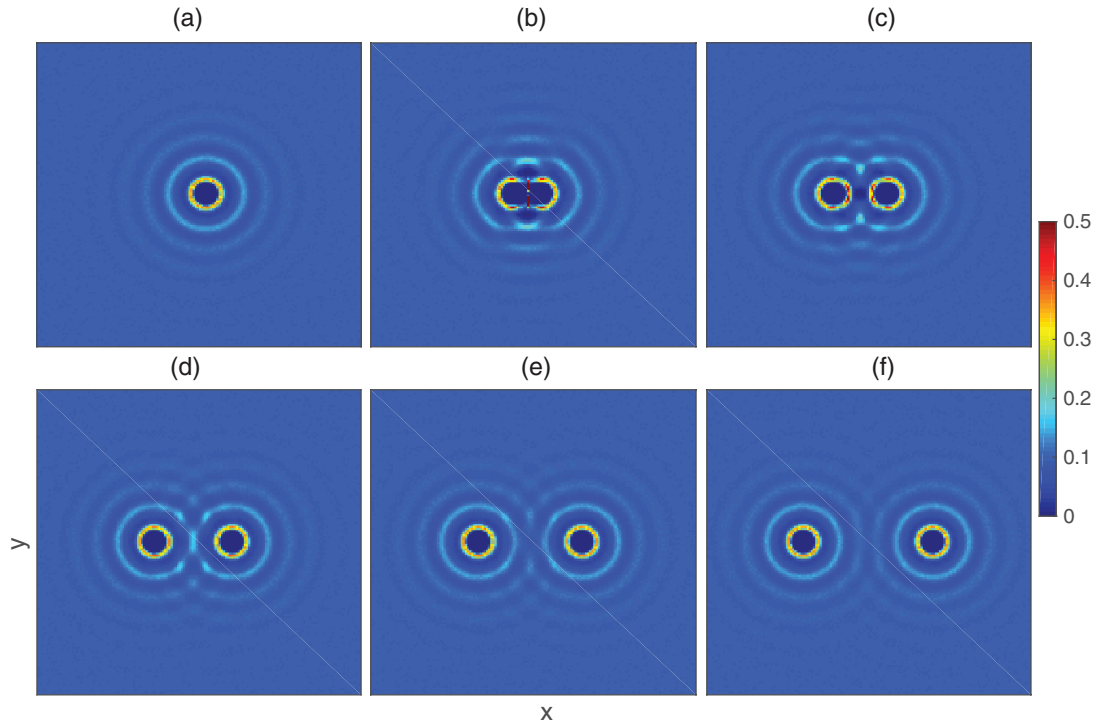
Figure 2. *Voronoi tessellations for pure system for a density ρ_0 with one and two pinned particles:* the averaged Voronoi tessellations for (a) a single pin, and two pins separated by $r = a, 2a, 3a, 4a, 5a$ are shown in (b)–(f) respectively. These simulations are for the density value $\rho_0 = 0.8$.
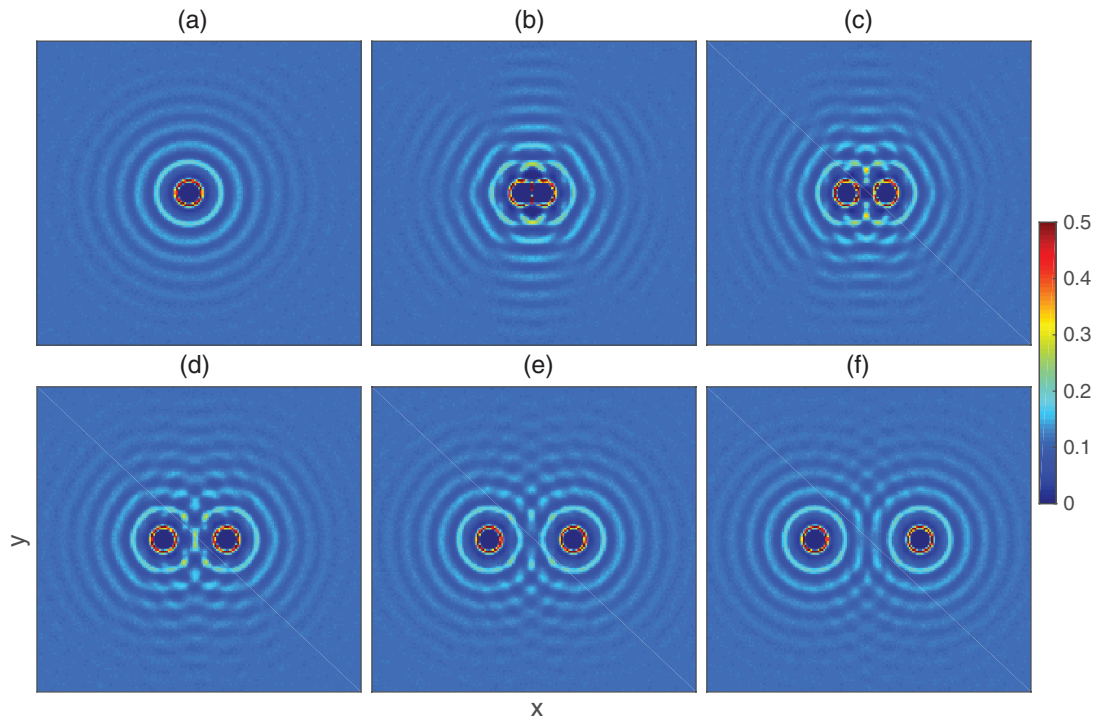

Figure 3. *The Voronoi tessellations for pure system for a density ρ_0:* the averaged Voronoi tessellations for (a) a single pin, and two pins separated by $r = a, 2a, 3a, 4a, 5a$ are shown in (b)–(f) respectively. Parameters: $\rho_0 = 0.95$.
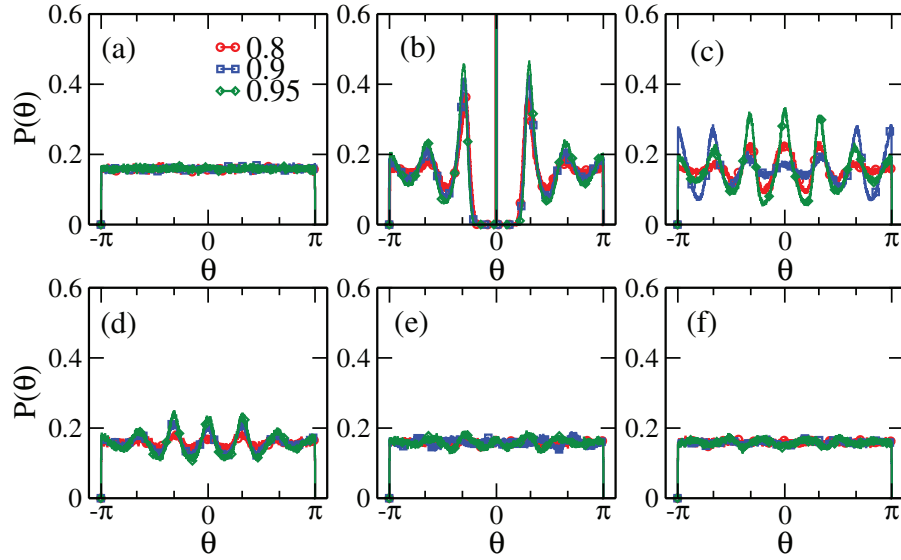
Figure 4. *The probability distribution of the angle in the first neighbour shell for various densities ρ_0:* the normalized probability distribution $P(\theta)$ of the angle θ subtended by the line joining a central pinned particle to a neighbour in the first neighbour shell, for sub-figure. (a) A single pin, where this angle is computed with respect to the x axis. Sub-figures. (b)–(f) Show the corresponding angle computed with respect to the axis formed by the line joining two pins separated by $r = a, 2a, 3a, 4a, 5a$. Data is shown for densities $\rho_0 = 0.8, 0.9, 0.95$.
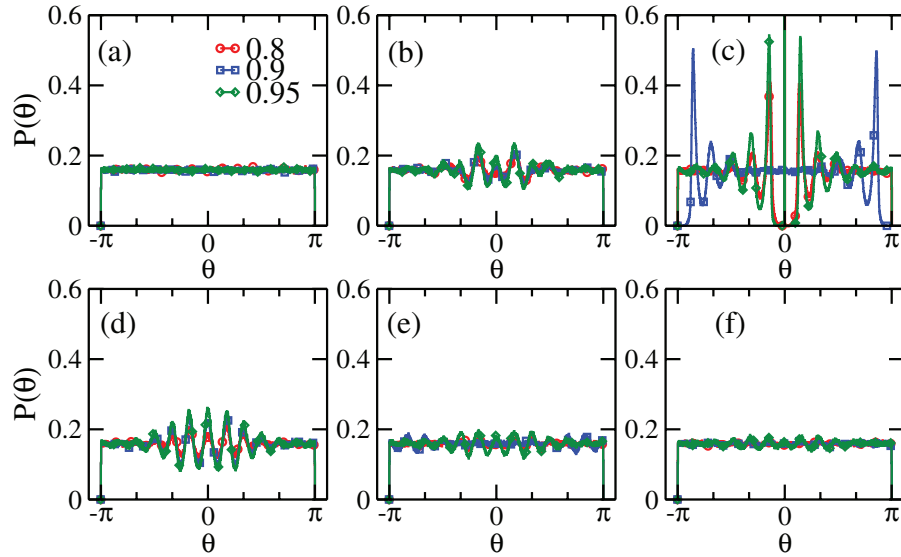

Figure 5. *The probability distribution of the angle in the second neighbour shell for various densities ρ_0:* the normalized probability distribution $P(\theta)$ of the angle θ subtended by the line joining a central pinned particle to a neighbour in the second neighbour shell, for sub-figure (a) a single pin, where this angle is computed with respect to the x axis. Sub-figures (b)–(f) show the corresponding angle computed with respect to the axis formed by the line joining two pins separated by $r = a, 2a, 3a, 4a, 5a$. Data is shown for densities $\rho_0 = 0.8, 0.9, 0.95$.

of density modulations due to two separate non-interacting pinned particles.

In figure 3, we show results for the increased density $\rho_0 = 0.95$. It is clear that the density redistribution arising from the two pinned particles cannot be decomposed into independent pieces even at a separation of $r = 5a$. As correlations build up at larger densities, the effects due to the pinning of two particles is not simply additive.

3.3. The orientational neighbourhood of pinned particles: angular distributions

Our Voronoi tesselations, as discussed in section 2, are well adapted to investigating questions of the instantaneous orientational neighbourhood of pinned particles. In particular, we ask whether the structuring of the immediate neighbourhood induced by the presence of two nearby pinned particles might penetrate beyond their separation. We study these by
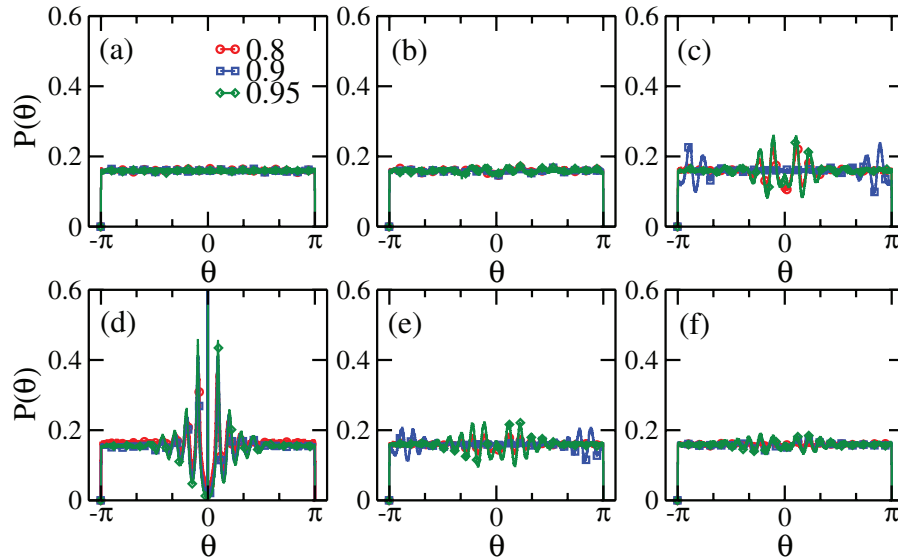
Figure 6. *The probability distribution of the angle in the third neighbour shell for various densities ρ_0:* the normalized probability distribution $P(\theta)$ of the angle θ subtended by the line joining a central pinned particle to a neighbour in the third neighbour shell, for sub-figure (a) a single pin, where this angle is computed with respect to the *x* axis. Sub-figures (b)–(f) show the corresponding angle computed with respect to the axis formed by the line joining two pins separated by $r = a, 2a, 3a, 4a, 5a$. Data is shown for densities $\rho_0 = 0.8, 0.9, 0.95$.

computing, using these tesselations, the probability of finding a particle at a fixed angle from a central pinned particle. For two pinned particles, this angle is computed relative to the line joining them. For a single particle, the choice of an axis is arbitrary.

We expect the following: for a single pinned particle, the probability of finding another particle oriented at angle θ from it, in either the first, second or even third neighbour shell, should be uniform. For two pinned particles, however, the line joining them serves as an axis picked out in an otherwise unstructured liquid. The fact that two particles are constrained to lie at a specific distance along this axis constrains other particles, which must now populate preferred orientations with respect to the two particles that lie along that line. Apart from density-driven commensurability effects that occur if the two particles are within 1–2 inter-particle spacings from each other, we expect that the neighbourhoods of the two particles must now be structured, with peaks in the angular distribution with a periodicity of $\pi/3$ and multiples thereof. As we consider shells of higher order, these angular correlations should become weaker until, asymptotically, they die out. We can extend this to the probability of finding a particle at a specific orientation in the first, second, third or even higher shell of neighbours.

Our results for the normalized probability distributions $P(\theta)$ of the angle θ for various densities ρ_0 in the first, second, and third neighbour shells are shown in figures 4 (first neighbour shell), 5 (second neighbour shell) and 6 (third neighbour shell) respectively. In the first neighbour shell, shown in figure 4, the distribution is uniform for the single pinned particle. Similar behavior is seen for higher order neighbour shells, as shown in figures 5(a) and 6(a). This is, of course, expected since the presence of a single pinning site does not bias the angular distribution of particles in its neighbourhood.

Our results for two pinned particles across different neighbour shells, with the particles separated by $r = a, 2a, 3a, 4a$ and $5a$ are shown in figures 4(b)–(f), 5(b)–(f) and 6(b)–(f). For pins separated by $r = a$, as in figures 4(b), 5(b) and 6(b), the probability of a fluid particle appearing in-between them is suppressed for purely steric reasons. However, there are other prominent peaks separated by an angle of $\pi/3$ that appear in the angular probability distribution, pointing to a well-defined orientational neighbourhood.

As the separation of the pinned particles is increased, through $r = 2a, 3a, 4a$ and $5a$, the peaks in the nearest neighbour shell are suppressed, as shown in figures 4(b)–(f). The peaks are most strongly suppressed for the lowest densities. As the density is increased, the periodic oscillations in $P(\theta)$ that are an indication of a well-formed angular neighbourhood become more prominent. They are only indistinguishable from the single pin case when particles are separated by more than about 4–5 inter-particle spacings.

Similar considerations hold for the higher-order neighbour shells. Commensurability effects lead to a large signal in the second neighbour distribution for $r = 2a$ (figure 5(c)). This signal is suppressed as the pinned particles are progressively separated. A similar commensurability is seen for the third neighbour shell for particles separated by 3a. Oscillations in the orientation of the neighbouring particles are prominent even at separations of $r = 4a$.

4. Summary and conclusions

In this paper, we first discussed the general problem of many-body correlations in a collection of particles in two dimensions that interact with a inverse twelfth power potential [49]. These particles, in addition, also experience a quenched, random one-body potential field with short-ranged correlations

[10–12]. We reproduced our earlier results for two point translational and orientational correlations in such a system, including those that calculated a new orientational correlation function, with non-trivial values only in systems of interacting particles with quenched disorder. The corresponding quantity involving positional correlations was studied earlier using a combination of liquid state theory, simulations and experiments [10–12].

In our earlier work, we found that that increasing quenched disorder enhanced medium-range orientational (hexatic) correlations in a liquid but destroyed it in a crystal. In this paper, we addressed this specific question, examining the suggestion that pairs of pinned particles might structure the neighbourhood around them so as to promote hexatic order. If the influence of these pairs of pinned particles could be propagated to larger scales, that would explain why quenched disorder plays such a counter-intuitive role in disordered fluids, acting both to suppress translational order while subtly enhancing orientational order, at least at intermediate scales accessible in simulations.

Our results indicated that the influence of a pair of particles pinned even at distances of about 4–5 inter-particle spacings could structure upto the third shell or more of neighbours about them in terms of hexatic correlations. We used Voronoi tesselations, as discussed in the earlier section, to first identify the instantaneous neighbourhood about pinned particles. This then enabled us to compute the orientational neighbourhood about these particles. We found that orientational anisotropies could persist over a length scale much larger than the particle separation.

Our physical picture of orientational order in correlated classical fluids in the presence of quenched disorder is thus the following. The ability for system-wide orientational structure to persist in a disordered interacting particle system in its fluid phase can only arise due to the presence, to lowest order, of a low density of pairs of well-pinned particles that are not too far away from each other. These structure their orientational neighbourhood even in the fluid. Because the orientational (hexatic) correlation length, even in the fluid, is large, the effect of such pinned pairs can be expected to persist for larger length scales than the pair separation. Other particles, even if far away, can adjust their positions so as to best align with these neighbourhoods. This could then potentially lead to hexatic order that could propagate weakly across a finite system, as seen in our simulations. We expect that quenched disorder cannot stabilize a long-ranged ordered hexatic phase, although there have been suggestions of a hexatic glass with related properties [50]. In contrast to that suggestion, we consider only the well-equilibrated fluid here.

We can suggest a number of additional directions that should be examined. The statistics of the minima of Gaussian random fields is one quantity that determines the probability of finding well-pinned particles proximate to each other. The study of effective field theories describing systems with short-to-medium-range hexatic order in the presence of specific types of correlated random fields might also provide useful insights into this problem.

To the best of our knowledge, the idea that local orientational order in two-dimensional fluids might be most affected by pairs of pinning sites that define local axes within the fluid, with such order percolating across short to intermediate scales, is new. Indeed, the presence of such strong local triangular order, induced by pinning, in a fluid system might be relevant to earlier observations of non-trivial three-body correlations in fluid and glassy phases of superconducting vortex systems [51]. We look forward to further experiments that might be able to test these ideas.

Acknowledgments

ORCID iDs

N Shankaraiah ⬤ https://orcid.org/0000-0001-9051-4686
Surajit Sengupta ⬤ https://orcid.org/0000-0002-3221-7437
Gautam I Menon ⬤ https://orcid.org/0000-0001-5528-4002

References

[1] Chaikin P and Lubensky T 1995 *Principles of Condensed Matter Physics* (Cambridge: Cambridge University Press)
[2] Kosterlitz M and Thouless D J 1973 *J. Phys. C: Solid State Phys.* **6** 1181
[3] Halperin B I and Nelson D R 1978 *Phys. Rev. Lett.* **41** 121 Nelson D R and Halperin B I 1979 *Phys. Rev.* B **19** 2457
[4] Young A P 1979 *Phys. Rev.* B **19** 1855
[5] Berezinskii V L 1971 *Sov. Phys.—JETP* **32** 493
[6] Hansen J P and Macdonald I R 1986 *Theory of Simple Liquids* (London: Academic)
[7] Giamarchi T and Bhattacharya S 2002 Vortex phases *High Magnetic Fields* (*Lecture Notes in Physics* vol 595) ed C Berthier *et al* (Berlin: Springer)
[8] Menon G I 2002 *Phys. Rev.* B **65** 104527
[9] Menon G I, Ravikumar G, Higgins M J and Bhattacharya S 2012 *Phys. Rev.* B **85** 064515
[10] Menon G I and Dasgupta C 1994 *Phys. Rev. Lett.* **73** 1023
[11] Sengupta A, Sengupta S and Menon G I 2005 *Europhys. Lett.* **70** 635
[12] Bewerunge J, Sengupta A, Capellmann R F, Platten F, Sengupta S and Egelhaff S U 2016 *J. Chem. Phys.* **145** 044905
[13] Sood A K 1991 *Solid State Phys.* **45** 1
[14] Arora A K and Tata B V R 1995 *Ordering and Phase Transitions in Charged Colloids* (New York: VCH)
[15] Löwen H 1994 *Phys. Rep.* **237** 76
[16] Ivlev A, Löwen H, Morfill G and Royall C P 2012 *Complex Plasmas and Colloidal Dispersions: Particle-Resolved Studies of Classical Liquids and Solids* (Singapore: World Scientific)

[17] Chen K, Kaplan T and Mostoller M 1995 *Phys. Rev. Lett.* **74** 4019

[18] Prestipino S, Saija F and Giaquinta P V 2005 *Phys. Rev.* E **71** 050102

[19] Qi W-K, Wang Z, Han Y and Chen Y 2010 *J. Chem. Phys.* **133** 234508

[20] Wierschem K and Manousakis E 2011 *Phys. Rev.* B **83** 214108

[21] Qi W, Gantapara A P and Dijkstra M 2014 *Soft Matter* **10** 5449

[22] Thorneywork A L, Abbott J L, Aarts D G A L and Dullens R P A 2017 *Phys. Rev. Lett.* **118** 158001

[23] Gasser U, Eisenmann C, Maret G and Keim P 2010 *Phys. Chem. Chem. Phys.* **11** 963

[24] Keim P, Maret G and von Grunberg H H 2007 *Phys. Rev.* E **75** 031402

[25] Deutschlander S, Horn T, Lowen H, Maret G and Keim P 2013 *Phys. Rev. Lett.* **111** 098301

[26] Horn T, Deutschlander S, Lowen H, Maret G and Keim P 2013 *Phys. Rev.* E **88** 062305

[27] Bernard E P and Krauth W 2011 *Phys. Rev. Lett.* **107** 155704

[28] von Grünberg H H, Keim P and Maret G 2007 *Phase Transitions in Two Dimensional Colloidal Systems, in Soft Matter* ed G Gommper and M Schick (New York: Wiley-VCH)

[29] Jaster A 2004 *Phys. Lett.* A **330** 120

[30] Zahn K and Maret G 2000 *Phys. Rev. Lett.* **85** 3656

[31] von Grünberg H H, Keim P, Zahn K and Maret G 2004 *Phys. Rev. Lett.* **93** 255703

[32] Prestipino S, Saija F and Giaquinta P V 2011 *Phys. Rev. Lett.* **106** 235701

[33] Chui S T 1983 *Phys. Rev.* B **28** 178

[34] Ramakrishnan T V 1982 *Phys. Rev. Lett.* **48** 541

[35] Ryzhov V N 1991 *Theor. Math. Phys.* **88** 990

[36] Ryzhov V N 1991 *Zh. Eksp. Teor. Fiz.* **100** 1627
Ryzhov V N 1991 *Sov. Phys.—JETP* **73** 899

[37] Ryzhov V N and Tareyeva E E 1995 *Phys. Rev.* B **1** 8789

[38] Ryzhov V N and Tareeva E E 1995 *Zh. Eksp. Teor. Fiz.* **108** 2044
Ryzhov V N and Tareeva E E 1995 *J. Exp. Theor. Phys.* **81** 1115

[39] Ryzhov V N, Tareyeva E E, Fomin Yu D, Tsiok E N and Chumakov E S 2017 *Theor. Math. Phys.* **191** 842

[40] Ryzhov V N and Tareyeva E E 2002 *Physica* A **314** 396

[41] Kapfer S C and Krauth W 2015 *Phys. Rev. Lett.* **114** 035702

[42] Hajibabaei A and Kim K S 2019 *Phys. Rev.* E **99** 022145

[43] Sengupta S, Nielaba P and Binder K 2000 *Phys. Rev.* E **61** 6294

[44] Zahn K, Wille A, Maret G, Sengupta S and Nielaba P 2003 *Phys. Rev. Lett.* **90** 155506

[45] Chudnovsky E M and Dickman R 1998 *Phys. Rev.* B **57** 2724

[46] Shankaraiah N, Sengupta S and Menon G I 2019 *J. Chem. Phys.* **151** 124501

[47] Edwards S F and Anderson P W 1975 *J. Phys. F: Met. Phys.* **5** 965

[48] Allen M P and Tildesley D 1987 *Computer Simulation of Liquids* (Oxford: Clarendon)

[49] Broughton J Q, Gilmer G H and Weeks J D 1982 *Phys. Rev.* B **25** 4651

[50] Roy I *et al* 2019 *Phys. Rev. Lett.* **122** 047001

[51] Menon G I *et al* 2006 *Phys. Rev. Lett.* **97** 177004